Original Research Article

GREENHOUSE GASES SCIENCE AND TECHNOLOGY

Microbial electrosynthesis for CO_2 conversion and methane production: Influence of electrode geometry on biofilm development

Celia De la Puente, Daniela Carrillo-Peña, Guillermo Pelaz, Antonio Morán and Raúl Mateos, Chemical and Environmental Bioprocess Engineering Group, Natural Resources Institute, University of León, León, Spain

Abstract: Electromethanogenesis is a process of microbial electrosynthesis (MES) in which electroactive microorganisms reduce carbon dioxide (CO_2) to produce methane (CH_4), using a cathode as an electron donor. The efficiency of this reaction is greatly determined by the establishment of a robust microbial community on the biocathodes, which eventually affects the global performance of the bioreactor. Moreover, the development of the biofilm depends on several characteristics of the electrodes, more specifically their material and geometry. Since electrode geometry is a crucial parameter, this study aims at evaluating the sole influence of the electrode shape by installing carbon-based electrodes with two different constructions (brush and carbon felt) of biocathodes in an electromethanogenic reactor for CO_2 capture. The overall performance of the reactors showed coulombic efficiencies around 100%, with high-quality biogas reaching methane concentrations above 90%. The results reveal that the electrode geometry affects the individual biocathode performance, and the carbon brush showed a bigger contribution to current generation and electrical capacitance, exhibiting higher peak hydrogen production compared to the carbon felt, which could be reflected in higher CO_2 capture and methane generation. Both geometries showed a greater proliferation of archaea over bacteria (between 53 and 85%), which was more significant on the brush than on the carbon felt. Archaea community was dominated by *Methanobacterium* in carbon felt electrodes and codominated with *Methanobrevibacter* in brush electrodes, while bacteria analyses showed a very similar community for both geometries.

Additional supporting information may be found online in the Supporting Information section at the end of the article.

Keywords: Biocathode; CO_2 capture; electroactive biofilm; electromethanogenesis; microbial electrosynthesis

Correspondence to: R. Mateos, Chemical and Environmental Bioprocess Engineering Group, Natural Resources Institute, University of León, León 24071, Spain.
E-mail: rmatg@unileon.es
Received June 21, 2022; revised September 16, 2022; accepted September 21, 2022
Published online at Wiley Online Library (wileyonlinelibrary.com). DOI: 10.1002/ghg.2185

Introduction

Industrial activity and nonrenewable energy consumption produced in 2021 the highest ever annual global CO_2 emissions level, which reached 36.3 gigatonnes.[1] The increasing atmospheric concentration of this greenhouse gas is rising the impact of global warming. CO_2 emissions are a difficult problem to solve, since the current technologies are not developed enough to be independent from fossil fuels in order to provide energy worldwide.[2] The utilisation and conversion of CO_2 into value-added products, namely chemicals and fuels, is an acknowledged option to address this challenge.[3–6]

One of the several emerging techniques using waste CO_2 is microbial electrosynthesis (MES), which refers to the electricity-driven reduction of CO_2 performed by electroactive microorganisms acting as biocatalysts.[4,7,8] MES systems consist of a bioreactor with an anode and a cathode immersed in a culture medium and separated by a membrane. Water oxidation takes place at the anode, while microbial CO_2 reduction occurs at the cathode.[7,9] Electron uptake by electrotrophic microorganisms growing on the surface of a solid cathode, or at its vicinity in planktonic form, is required for the cathodic reaction.[3,4,10] One of the most promising applications of MES technology is electromethanogenesis, which refers to bioelectrochemical methane production.[11] In this process, an electric current is supplied to electrotrophic microorganisms for the conversion of CO_2 into a high-purity biogas within the biocathode of a MES system.[12,13]

The biocathode is a solid electrode acting as an electron donor source for the biofilm that forms on its surface, hence it is one of the key components of a MES needed to achieve optimum performance.[12,14,15] The variety of electrode geometries and material properties plays a role on microbial adhesion, which affects the biofilm development and electron exchange.[12,16] As a consequence, the production rates of organic compounds are influenced as well.[17] Bioelectrode materials must have a high surface area and be biocompatible and chemically stable.[18] They should provide efficient electrical conduction and electron transfer capacity between the electrode and the biofilm.[19] Carbon-based materials are an economic option that meet these characteristics and provide a variety of manufacturing possibilities, including carbon paper, carbon cloth, carbon felt and carbon brush, among other novel alternatives such as gas diffusion electrodes.[13,20–24] It is known that the electrodes' geometric shape determines their internal resistance and affects the current distribution.[9] A recent study conducted in a bioelectrochemical system revealed that carbon felt electrodes produced lower power densities and presented higher resistances than brush electrodes, which demonstrates that the latter have a superior performance. In this particular case, the maximum power density was 2.35 ± 0.09 W·m^{-2} for the brush and 1.46 ± 0.01 W·m^{-2} for the carbon felt when used as anodes. Cathode potentials reached >7 A·m^{-2} when using a brush anode and <4.5 A·m^{-2} with a felt.[25] When used as cathodes in MES bioreactors, recent experiments have achieved a methane production rate of 52.8 ml·day^{-1} working with brush electrodes (2.5 cm diameter × 12.0 cm height) and 81.6 ml·day^{-1} with felt electrodes (10.0 cm × 6.8 cm), both studies carried out at 35°C.[26,27] However, given that the presented data were obtained independently from each other, their comparison might not be completely accurate. Moreover, only the bioreactor performance in terms of methane production is analysed. The biofilm growth on each type of electrode, which comprises a critical parameter to understand methane production and obtain high production rates,[28] is overlooked in those previous studies.

The aim of this work is to evaluate the effect of different geometries in a MES system used for carbon dioxide capture and methane production, studying the development of electroactive biofilms, their electrochemical behaviour and bioreactor performance.

Materials and methods

MES reactors setup

The MES experiments were carried out in two different double-chamber H-cell reactors (Adams & Chittenden, USA) acting as replicates with a working volume of 0.5 L per chamber, separated by a cation exchange membrane (CMI-7000, Membranes International Inc.) and connected in a three-electrode configuration. These reactors will be referred to as R1 and R2 throughout the manuscript. The cathode chamber was connected to a gas collection bag through a modified cap, which allowed the passive diffusion of CO_2 from the gasbag to the reactor. In the anode chamber a platinum mesh (1.5 × 1.5 cm) was placed as a counter-electrode (CE), while in the cathode chamber,

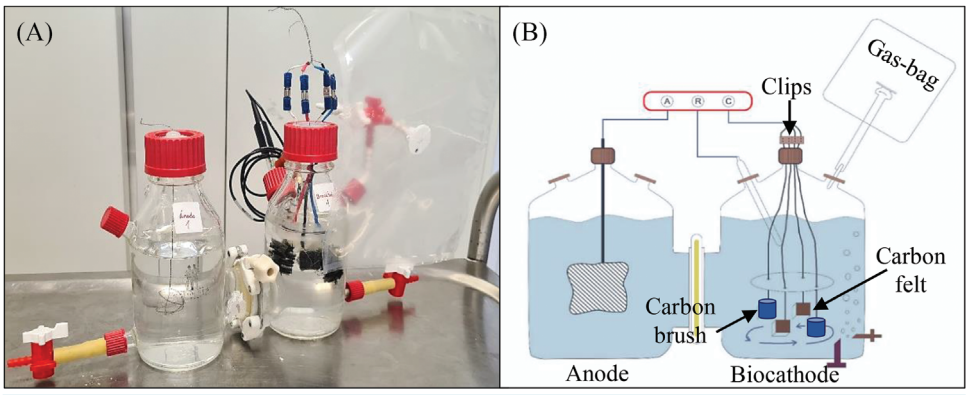

Figure 1. Microbial electrosynthesis reactor (H-Cell MES): (A) actual reactor assembly and (B) reactor configuration scheme.

an Ag/AgCl (3 M KCl) electrode (RE; Sigma-Aldrich® glass reference electrode, glass 12 mm) was used as a reference and four carbon-based electrodes with different geometry were placed as working electrodes (WE) inside the same chamber. Two of them were carbon felts (1.5 cm x 1.5 cm x 0.5 cm) and the two others were carbon brushes (2 cm diameter x 3 cm height), with an apparent surface (AS) of 2.25 cm2 and 5.33 cm2, respectively. These AS have been calculated as a rectangular area in the case of carbon felt and according to Mateos et al. (2017) in the case of carbon brush, as explained in Supporting Information Section S1.[18] The two types of electrodes were in duplicate to ensure the accuracy of the statistical results, calculating the mean and standard deviation of sampling variables, and normalising the performance to each electrode apparent area. For R1, the electrodes will be referred to as $TF1_{R1}$–$TF2_{R1}$ (carbon felts) and $B1_{R1}$–$B2_{R1}$ (brushes). In R2, they will be identified as $TF1_{R2}$–$TF2_{R2}$ (carbon felts) and $B1_{R2}$ and $B2_{R2}$ (brushes). Titanium wire was attached to each electrode and covered by heat-shrinkable plastic tubes to avoid any contact between the electrodes or with the reference. The WEs were kept in place by a chemically inert silicone structure. On the outside, they were connected and combined to a working electrode lead of the potentiostat, as shown in Fig. 1. This configuration was designed to carry out the bioelectrochemical experiments. It also allowed individual measurements of the current consumed by each electrode. For these measurements, the WE were subsequently disconnected from the combined cable and directly connected to the potentiostat to determine their individual contribution.

Inoculation and experimental phase

The inoculum was taken from a cathodic chamber of a CH_4-producing microbial electrosynthesis reactor that was operated for approximately 300 days in our laboratory.[12] The cathode chamber was filled with 70% (v/v) inoculum and 30% (v/v) synthetic medium (SM) supplemented with 0.5 g·L^{-1} of $NaHCO_3$, 200 ml of CO_2 and 100 ml of H_2. The SM contained: 3.2 g·L^{-1} K_2HPO_4, 1.6 g·L^{-1} KH_2PO_4, 0.28 g·L^{-1} NH_4Cl, 0.0075 g·L^{-1} $CaCl_2$, 0.01 g·L^{-1} $MgSO_4$, 0.09 g·L^{-1} $MgCl_2$, 1 ml of vitamin solution and 1 ml of mineral solution per litre, as described by Van Eerten-Jansen et al.[29] The inoculum and SM mixture was bubbled with N_2 gas for 30 min to ensure anoxia, and afterwards the CO_2 and H_2 gas mixture was added on the reactor. A second cycle named re-inoculation was performed using the same conditions as the previous one. The microbial reinoculation was conducted to strengthen the microbial community attachment and colonisation of the carbon electrode surface. The anode chamber was filled with the same SM without vitamins or carbon sources to avoid microorganism growth while maintaining ion balance between chambers. The inoculation was carried out for 14 days and ended when a stabilisation in the electrical current and an evolution in the methane present in the biogas were observed.

The experimental phase consisted of 10 cycles in batch mode (7 days per cycle), using only CO_2 gas (300 ml) as the carbon source in 100% SM without the previous presence of bicarbonate, and replacing the SM completely between cycles. It was performed at a constant temperature (30°C) by means of a magnetic hot plate stirrer that regulated the temperature with a

stirring velocity of 270 rpm (MS-H-S10, Scilogex). Twice per cycle (at the highest current peak and at the end of the cycle) the electrodes were randomly disconnected using the clips at the top to determine the individual contribution of each electrode to the generated current.

Electrochemical and analytical measurements

The bioelectrochemical analysis was carried out using a biologic VSP multichannel potentiostat (software EC lab vs. 11.36) in a three-electrode configuration including chronoamperometry (CA) and cycle voltammetry (CV) techniques. During the CA tests in the inoculation and experimental phase, the biocathodes were polarised at −1 V (vs. Ag/AgCl) and the current production was monitored every 600 s. CV tests were performed at the end of every cycle (starving condition) to characterise the biofilm growth on each WE with a potential range of −1.0 V to 0.1 V vs. RE (scan rate: 5.0 $mV{\cdot}s^{-1}$). The composition of the biogas was determined at the end of each cycle using a gas chromatograph (Varian CP3800 GC) equipped with a thermal conductivity detector (TCD) in terms of hydrogen (H_2), carbon dioxide (CO_2), carbon monoxide (CO), oxygen (O_2), nitrogen (N_2) and methane (CH_4). The reactors were bubbled with nitrogen for 30 min at the beginning of each cycle. The amount of nitrogen present in the headspace at the start of each cycle remains inside the reactor and is deducted from the gas recovered at the end of the cycle.[30]

In the liquid sample, redox (pH-Meter, pH 91; Wissenschaftlich Technische Werkstätten, WTW), pH (pH-Meter BASIC 20+, Crison), dissolved oxygen and conductivity (Hach, HQ40d - two-channel digit multimeter) measurements were monitored following standard methodologies.[31] Total organic carbon (TOC), total inorganic carbon (IC) and total nitrogen (TN) were measured using an analyser (multi N/C 3100, Analytikjena).

Microbial community analysis

A scanning electron microscopy (SEM) test was performed to characterise the morphology surface of the carbon felt and bristles of brush electrodes before and after biofilm fixation (abiotic electrodes and bioelectrodes at the end of cycle 10). Sample preparation was carried out as described above by fixing the electrode/microorganisms in 2.5% glutaraldehyde in phosphate-buffered sterile solution for 1 h at room temperature; the samples were washed and kept at 4°C overnight.[32] They were later dried using the Leica EM CPD300 critical point dryer, placed onto specimen mounts with contact adhesive and covered with colloidal gold by the Leica EM ACE200 Vacuum Coater. Samples were visualised with a JEOL JSM 6100 scanning electron microscope and digitally captured.

DNA extraction was done also from the surface (carbon felt) and bristles (brushes) of the biocathodes, for which approximately 300 mg of sample were cut. These samples were used to characterise the microbial community developed on the electrodes surface at the end of the experiment (cycle 10). The microbial communities were analysed and followed along the experimental time by high throughput sequencing of massive 16S rRNA gene libraries. Total bacteria and archaea were analysed. Genomic DNA was extracted with a DNeasy PowerSoil Kit (Qiagen) according to the manufacturer's instructions. All PCR reactions were carried out in a Mastercycler (Eppendorf, Hamburg, Germany), and the PCR samples were checked for the size of the product on a 1% agarose gel and quantified by a NanoDrop 1000 (Thermo Scientific). The entire DNA extract was used for high-throughput sequencing of 16S rRNA gene-based libraries with 16S rRNA gene-based primer for bacteria 515F-806R and a specific primer for archaea 349F-806R. The Novogene Company (Cambridge, UK) carried out Illumina sequencing using a HiSeq 2500 PE250 platform.

The DNA readings obtained were compiled in FASTq files for further bioinformatics processing, carried out using QIIME software, version 1.7.0.[33] Sequence analysis was performed by the Uparse software (v7.0.1001) using all the effective tags. Sequences with ≥97% similarity were assigned to the same operational taxonomic units (OTUs). The representative sequence for each OTU was screened for further annotation. For each representative sequence, Mothur software was used against the SSUrRNA database of the SILVA database, for species annotation at each taxonomic rank (threshold: 0.8–1).[34]

The quantitative analysis of all samples was carried out by means of the quantitative-PCR reaction (qPCR) using a PowerUp SYBR Green Master Mix (Applied Biosystems) in a StepOnePlus Real-Time PCR system (Applied Biosystems). The qPCR amplification was performed for the 16S rRNA gene, in order to quantify the entire eubacteria community and for the mcrA

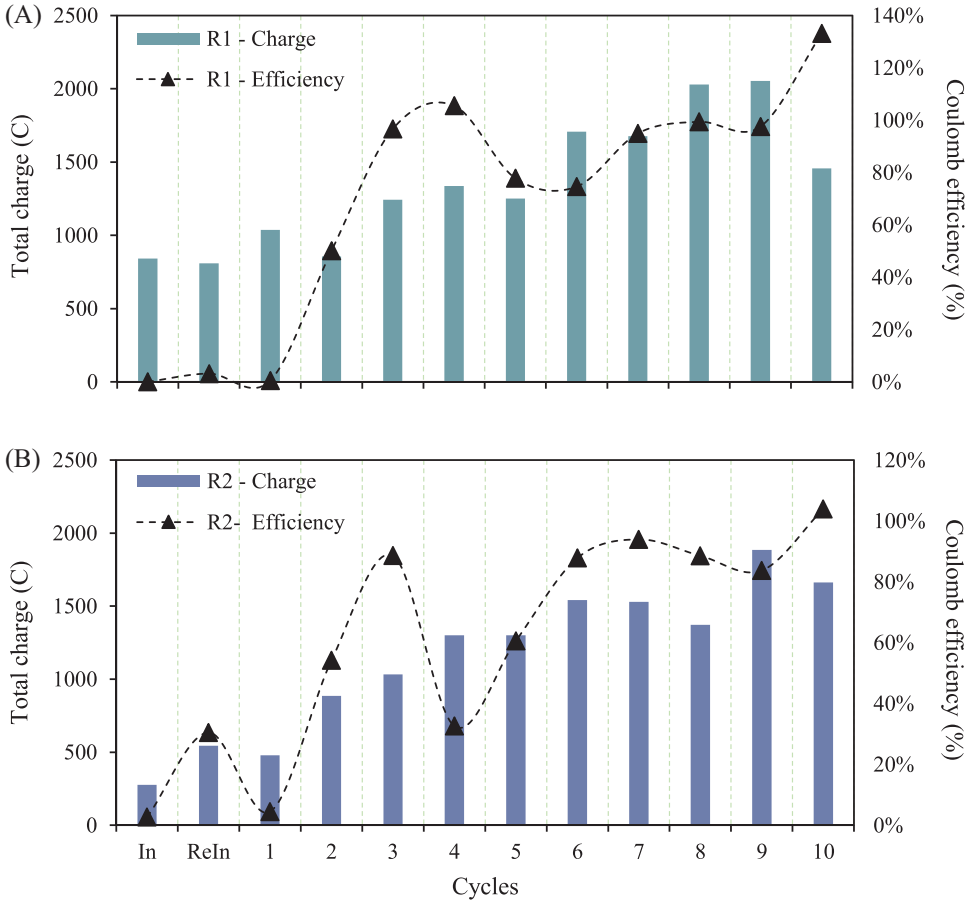

Figure 2. Total charge and coulomb efficiency during the inoculation and experimental phase for (A) R1 and (B) R2 separately.

gene, to quantify the total methanogen community. The primer set 314F qPCR (5′-CCTACGGGAG-GCAGCAG-3) and 518R qPCR (5′-ATTACCGCGG-CTGCTGG-3′) at an annealing temperature of 60°C for 30 s was used for bacteria, and Arc 349F (5′-GYGCASCAGKCGMGAAW-3′) and Arc 806R (5′-GGACTACVSGGGTATCTAAT-3′) for archaea quantification.

Results and discussion

Global reactor performance

Both reactors showed evident replicability, developing similar general performances during the entire experimental period. Figure 2 shows the total charge and coulomb efficiency for R1 and R2 during the experimental phase. Total transferred charge during the experimental phase increased proportionally as the cycles progressed, with a similar trend in both reactors. This behaviour demonstrates the growth of the microorganisms and the establishment of an electroactive biofilm on the biocathode surface, probably due to the reduction processes taking place.[9] The reactors show low variability from cycle 6 onwards, reaching the maximum total load at cycle 9 with 1884.6 C and 2054.2 C for R1 and R2, respectively.

The coulombic efficiency for all cycles was calculated considering the two possibly valuable products present which are methane and hydrogen. The coulombic efficiencies and total loadings shown at the beginning of the experimentation in both reactors (from inoculation to cycle 2) are due to the fact that the methanogenic biofilm is just starting to develop and the methanogenic communities in the system are poorly adapted, which is consistent with the absence of methane in the biogas during this stage (see Fig. 3).[35] The coulombic efficiency of the system starts to be significant from cycle 3 in both reactors, when methane is observed in the biogas composition. This efficiency is variable during the experimentation time,

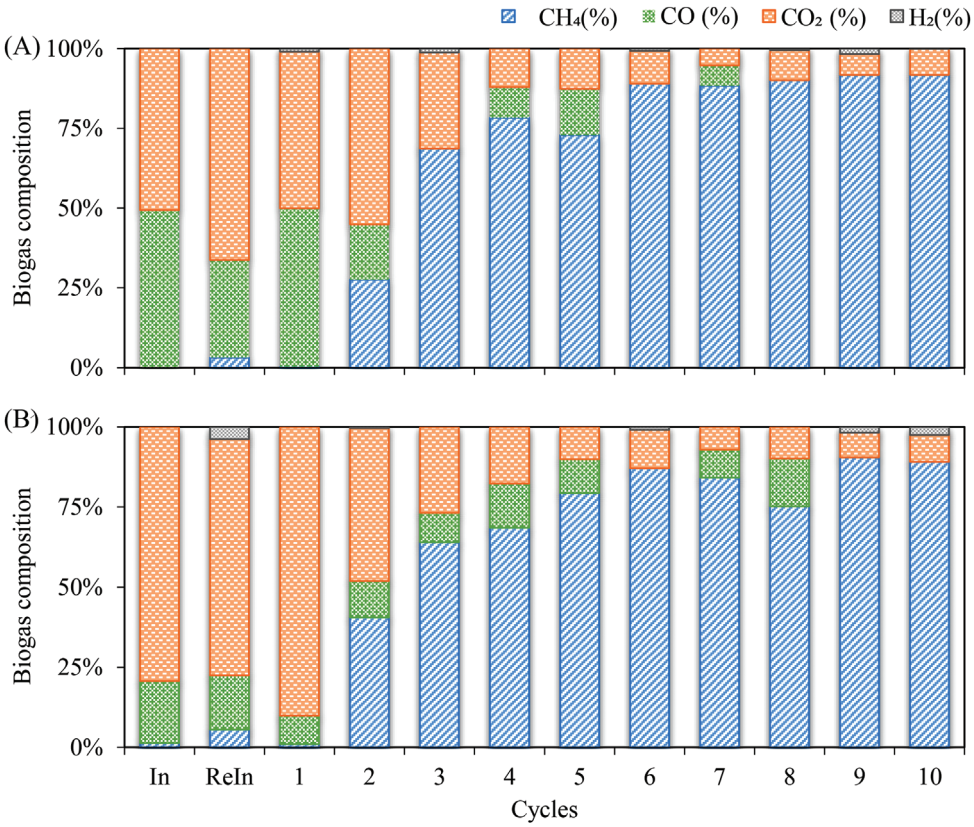

Figure 3. Biogas composition during the experimental phase for (A) R1 and (B) R2.

but for R1 there is a stabilisation stretch between cycle 7 and 9 at 97.3% ± 1.8% and R2 presents the same behaviour between cycle 6 and 9 with efficiencies around 88.5% ± 3.6%. However, in cycle 10, efficiencies higher than 100% are observed in both reactors, behaviour that could be due to the degradation of the dead biomass, used as an additional carbon source for methane synthesis.[36] This hypothesis could be supported by the decline in the total charge consumed by the biofilm during this cycle. A well-established electroactive biofilm requires less energy for the metabolic functions than the growing microbial community in the inoculation phase, when the electrons consumed were directed towards the stabilisation of the biofilm on the cathode.[37] This could explain the higher coulombic efficiency obtained in the experimental phase compared to the inoculation phase.

Figure 3 shows the biogas composition for reactors R1 and R2 during the process. As mentioned above, from cycle 2 onwards, the presence of methane in the biogas is observed, which could be related to the biofilm development. However, from cycle 6 onwards, in which it could be deduced that its electroactive biofilm has developed, a high selectivity with low variability in methane composition is observed, reaching average values of 90.2% ± 1.4% for R1 and 84.7% ± 5.2% for R2. It is interesting to underline the large amount of CO present in the biogas during the first experimentation cycles, especially in R1. CO is a reduction product of CO_2, which can react with H_2 to form CH_4.[38] Since the methanogenic population did not seem to be relevant until after cycle 3, CO reduction was not noticeable until then. H_2 was only present in some cycles and in very low concentrations (<3%). H_2 production was probably biologically induced, and this molecule could mediate the flow of electrons from the electrode to CO_2.[39] Several different mechanisms probably contributed to the methane production.

Individual behaviour of the electrodes

The individual disconnection of the WE determined its percentage contribution to the electric current. These results were calculated using the current density in order to compare both geometries, since they are

different in terms of apparent surface area. Both reactors had a carbon brush electrode with a considerably higher electrical current contribution than the other electrodes. For R1 the $B1_{R1}$ electrode accounts for about 43.2% ± 4.7% and in R2 the $B1_{R2}$ brush had 44.0% ± 11.4%. However, in both bioreactors the contribution of the remaining brush was remarkably inferior, $B2_{R1}$ and $B2_{R2}$ showing values of 26.2% ± 3.7%, and 15.5% ± 6.4%, respectively. In contrast, the carbon felt electrodes behaved similarly in each reactor, that is, with no major differences between them. For R1, $TF1_{R1}$ and $TF2_{R1}$ contribute 16.8% ± 3.8% and 13.8% ± 4.1%, respectively and in R2, $TF1_{R2}$ and $TF2_{R2}$ have a contribution of 19.6% ± 4.2% and 20.9% ± 9.6%, respectively. For more details, see Table S2 in the Supporting information document.

The conjoined contribution of both brushes of each reactor is superior to the sum of the corresponding felt electrodes. In R1, the brush electrode with the lowest percentage still provides a higher contribution than the best carbon felt electrode. The average recorded current density for the brush electrodes was -1.51 $A{\cdot}m^{-2}$ in R1 and -1.18 $A{\cdot}m^{-2}$ in R2. For the felt electrodes, the average current density recorded was -0.74 $A{\cdot}m^{-2}$ for R1 and -0.79 $A{\cdot}m^{-2}$ for R2. Since the current consumption is associated with biofilm development,[37] the brush electrodes proved to be better in terms of microbial growth as they have a higher current density.

The CV results obtained for each electrode within R1 and R2 during the experimental stage are shown in Fig. 4. A favourable evolution in terms of current generated is observed for all electrodes when comparing each electrode at the beginning (abiotic condition) and at the end of the test (electrodes with a developed biofilm) in Figs. (4A, B, D, and E). This evolution is evidenced by the increased space between the oxidation and reduction voltammetry curves and the presence of oxidation and reduction peaks at the end of cycle 10. These results are comparable with other authors who showed the same behaviour, in which a biofilm development or growth was deduced compared to the initial stages of the study.[40–42]

Figures (4C and F) compare a brush and a carbon felt belonging to R1 and R2, respectively. It can be seen that for both reactors the capacity (the space between the oxidation and reduction voltammetry curves) of the brushes is much higher than the carbon felt, indicating a great difference between the two types of geometry. At -1.0 V is the peak corresponding to the hydrogen evolution reaction (HER),[43] and it can be seen that this peak is considerably higher in the brush compared to the carbon felt for both reactors. This is relevant since methane production could be carried out by the hydrogenotrophic pathway and a larger peak would indicate a higher hydrogen generation that can promote a higher methane production ($4H_2 + CO_2 \rightarrow CH_4 + 2H_2O$).[12,13,44] Possibly, the specific brush geometry favours the growth of the biofilm and thus the adhesion of microorganisms to it. The brush geometry provides good mass transport and has a lower risk of clogging. On the other hand, thick carbon felt electrodes have large ion diffusion and electron conduction lengths. This is a drawback for electrodes colonisation, as it prevents a bioelectrochemical contribution from the inner structure of the electrodes.[17]

Microbial community analysis

Figure 5 shows the SEM images of the electrodes at the beginning and at the end of the experiment (cycle 10). The microstructure of the electrodes differs slightly between the geometry of the carbon brush and the carbon felt, as shown in Figs (5A and D), respectively. The brush is made of cylindrical fibres, while the structure of the carbon felt appears to show a different extrusion pattern. The irregular structures on the surface of the abiotic fibres could correspond to manufacturing imperfections or remaining dust particles. Figures (5B and E) show the images of the colonised brush and carbon felt, respectively. The abundance of rod-shaped microorganisms of different lengths on both electrode geometries, and especially the presence of microorganisms of more than 15–20 μm in length, which could act as an electroactive bridge between two nearby clusters of microorganisms, is noteworthy (Figs 5C and F). Extracellular polymeric substances (EPS), a complex high-molecular-weight mixture of polymers produced by microorganisms,[45] can also be observed among the cells. EPS produced by electroactive strains possess redox capabilities, which could facilitate extracellular electron transfer.[46] However, other major differences can be seen in the microbiological characterisation presented in the following sections.

Figure 6 shows the quantitative analysis (qPCR) of the bacterial and archaeal populations of a brush and a carbon felt for each reactor. Both geometries were dominated by archaea over bacteria (53–85% more). Also, in both reactors, higher gene archaea copies were

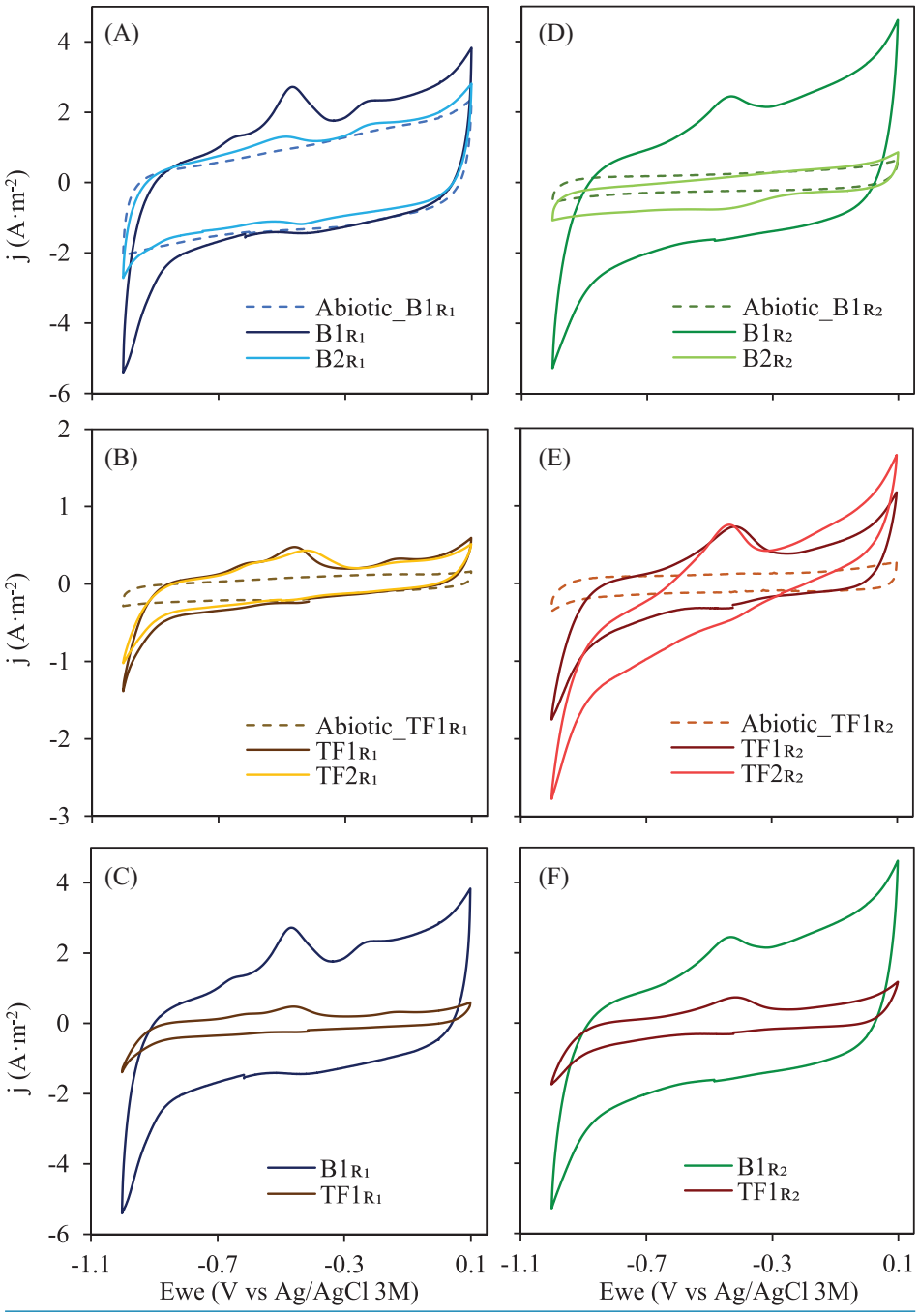

Figure 4. Cyclic voltammetries for: R1 with (A) brushes ($B1_{R1}$ & $B2_{R1}$) and abiotic electrodes, (B) carbon felts ($TF1_{R1}$ & $TF2_{R1}$) and abiotic electrodes and (C) comparison between $B1_{R1}$ and $TF1_{R1}$; and R2 with (D) brushes ($B1_{R2}$ & $B2_{R2}$) and abiotic electrodes, (E) carbon felts ($TF1_{R2}$ & $TF2_{R2}$) and abiotic electrodes and (F) comparison between $B1_{R2}$ and $TF1_{R2}$.

observed in the brush electrodes compared to the carbon felt, 35% ($B1_{R2}$) and 39% ($B1_{R1}$) more for R1 and R2, respectively. However, the behaviour of the bacteria was different, with a slightly higher abundance of bacteria in the carbon felt compared to the brush. It could be suggested that the brush geometry favours the proliferation of archaea over the felt geometry, which is essential for the methane-producing reactor.

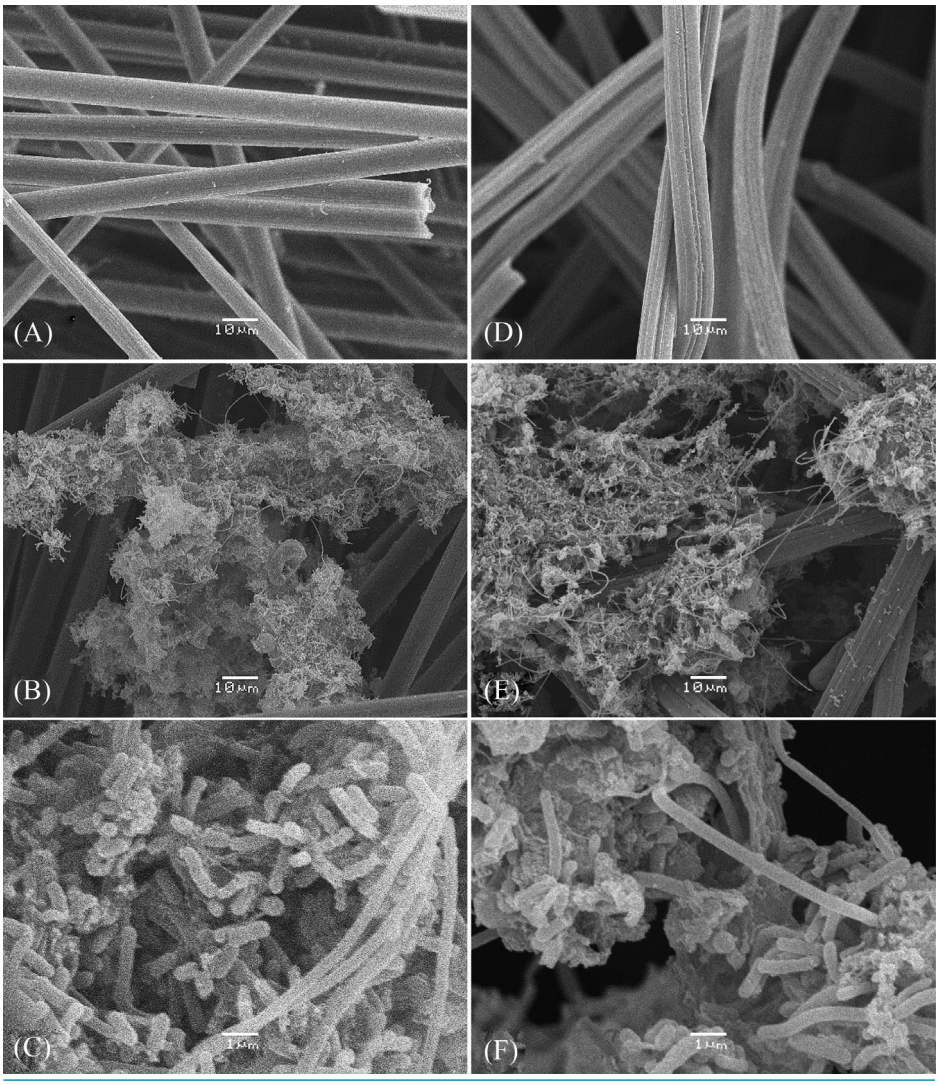

Figure 5. SEM images showing (A) abiotic brush and (B, C) colonised brush compared to (D) abiotic carbon felt and (E, F) colonised carbon felt.

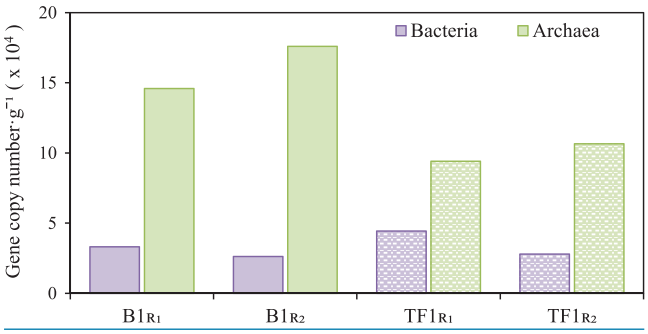

Figure 6. Gene copy number in terms of bacteria and archaea in a brush and felt electrode of each cathodic chamber.

Microbial community analyses show differences between brush and felt electrodes for both archaea and bacteria. Main genera, families and phyla present over 1% within the community are discussed, categorising the rest as "others."

Regarding archaea, the biofilms were dominated by hydrogenotrophic methanogenic archaea, mainly *Methanobacterium* and *Methanobrevibacter* which are members of the *Methanobacteraceae* family.[47] Carbon felts showed a higher relative abundance of *Methanobacterium*, with 73.0% for $TF1_{R1}$ and 72.5% for $TF1_{R2}$; whilst *Methanobrevibacter* represented approximately 26% for both electrodes. The behaviour of brush electrodes was slightly different from the TF electrodes as the relative abundances of

Table 1. Taxonomic classification of 16S rDNA Amplicon Sequencing gene from Archaea at genus level.

Archaea at genus level	$B1_{R1}$	$B1_{R2}$	$TF1_{R1}$	$TF1_{R2}$
Methanobacterium	45.3%	60.1%	73.0%	72.5%
Methanobrevibacter	52.6%	38.0%	25.9%	26.1%
Others	2.1%	1.9%	1.1%	1.4%

Methanobacterium and *Methanobrevibacter* were similar as shown in Table 1. *Methanobacterium* is able to produce CH_4 from CO_2 as a carbon source and H_2 as an electron donor,[48] and it is usually found in high abundance in biocathodes destined for methane production.[11] The direct electron transfer between species has also been studied, in which certain strains of *Methanobacterium* accept electrons from different bacteria.[49] The increased abundance of *Methanobrevibacter* in brush electrodes might be explained by its higher current consumption. It is possible that more negative potentials favour the synthesis of toxic by-products like hydroxyl radicals and peroxides, being *Methanobrevibacter* more adapted for its degradation.[47] The similar presence of both genera in the brush electrodes shows a more versatile community which might be the reason for their higher current consumption. Other studies on biolectrochemical systems have also found *Methanobrevibacter* as a predominant genus involved in the methanogenesis process.[29,47,50]

The microbial community in terms of bacteria showed a higher diversity compared with archaea. Both geometries were mostly dominated by Proteobacteria (35–40%), Chloroflexi (18–42%) and Bacteroidetes (6–17%) which are common phylum found in electromethanogenesis systems.[35,51–55] See Supporting information Fig. S2.

Figure 7 shows the taxonomic classification bacteria at genus level for the electrodes in reactors R1 and R2. *Paracoccus* genus represented a high percentage of the total bacteria in all biocathodes (17–10%). Previous studies have confirmed its ability of extracellular electron transfer based on its abundance in the biofilm zones closest to the electrode.[56] *Paracoccus*, as well as *Aquamicrobium*, *Xanthobacter* and *Hydrogenophaga*, could reduce nitrogen and some of them CO_2 to biomass.[57–59] A high concentration of the A4b family has also been found in the brushes and felts operated in

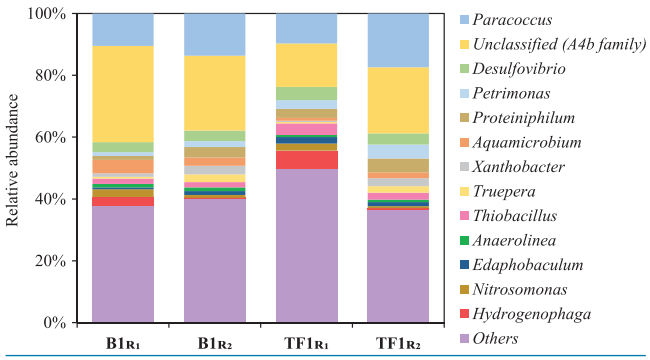

Figure 7. Taxonomic classification of 16S rDNA Amplicon Sequencing gene from Bacteria at genus level.

this study, which is Chloroflexi-like filamentous bacteria.[60] This family is represented by a unique unclassified genus, which is reported to be involved in ammonia oxidation, leading to loss of nitrogen.[60]

The genus *Petrimonas* was found in all geometries and they have been previously described in reactors for methane production,[61] which highlights its relevance in this type of systems. The genus *Proteiniphilum* has been identified in anaerobic reactors as a producer of volatile fatty acids (VFAs) by anaerobic fermentation, maintaining syntrophic relationships with VFA-degrading microorganisms and hydrogenotrophic methanogens.[62] The VFA produced could be used for methane production and that is why no organic matter is found at the end of the cycles.

Hydrogen production can be explained by the presence of *Desulfovibrio*, which has several cytochromes that facilitate the transport of electrons from the electrode to a hydrogenase enzyme. This enzyme catalyses H_2 synthesis at the cathodes, leading to a coulombic efficiency close to 100%.[63,64]

Conclusions

The system described in this work was able to produce methane from captured CO_2. Once the electroactive biofilm has developed, efficient microbial electrosynthesis is achieved. Both reactors produce high-quality biogas in which methane accounted for around 90% of the total composition. Regarding the different geometry of the electrodes, it has been observed that the brush is superior to felt in terms of current generated and, presumably, also in methane production. Improved electrical capacity and better hydrogen production peaks are also exhibited in the brush geometry over the felt geometry.

The colonisation of all electrodes is visible, although the carbon brush structure enhanced the initial attachment of the microorganisms and the subsequent biofilm formation. In addition, the operating conditions established in these reactors favour the proliferation of archaea, especially in the brush, while the number of bacteria is similar for both geometries. The carbon felts carry out the methanogenic process mainly by the presence of *Methanobacterium*. However, brush electrodes have a more versatile structure as they include microorganisms of the genus *Methanobacterium* and *Methanobrevibacter*, which could be the reason for their larger current consumption, resulting in a higher methane production. Bacteria analyses in both geometries showed similar communities.

Acknowledgements

This research was possible thanks to the financial support of the "Ministerio de Ciencia e Innovación (Gobierno de España)" project ref.: PID2020-115948RB-I00-TMA funded by MCIN/AEI/10.13039/501100011033.

References

1. International Energy Agency. Global energy review: CO_2 emissions in 2021. Paris; 2022.
2. Martens JA, Bogaerts A, De Kimpe N. et al. The chemical route to a carbon dioxide neutral world. ChemSusChem. 2017;10(6):1039–55.
3. Mateos R, Escapa A, Vanbroekhoven K, Patil SA, Moran A, Pant D. Microbial electrochemical technologies for CO_2 and its derived products valorization. In: Mohan SV, Varjani S, Pandey A, editors. Microbial electrochemical technology. Amsterdam, the Netherlands: Elsevier; 2019:777–96.
4. Bian B, Bajracharya S, Xu J, Pant D, Saikaly PE. Microbial electrosynthesis from CO_2: challenges, opportunities and perspectives in the context of circular bioeconomy. Bioresour Technol. 2020;302:122863.
5. Dağlıoğlu T, Öğüt TC, Ozdemir G, Azbar N. Comparative analysis of the effect of cell immobilization on the hydrogenothrophic biomethanation of CO_2. Greenh Gases Sci Technol. 2021;11:493–505.
6. Mishra S, Raghuvanshi S, Gupta S. Carbon dioxide to bio-fuels by mixed and pure microbial cultures isolated from activated sludge: relative evaluation of CO_2 fixation, biodiesel production, and thermodynamic analysis. Greenh Gases Sci Technol. 2019;9:1135–57.
7. Rabaey K and Rozendal RA. Microbial electrosynthesis - Revisiting the electrical route for microbial production. Nat Rev Microbiol. 2010;8(10):706–16.
8. Nevin KP, Woodard TL, Franks AE, Summers ZM, Lovley DR. Microbial electrosynthesis: feeding microbes electricity to convert carbon dioxide and water to multicarbon extracellular organic compounds. MBio. 2010;1(2). https://doi.org/10.1128/mBio.00103-10
9. Sharma M, Alvarez-Gallego Y, Achouak W, Pant D, Sarma PM, Dominguez-Benetton X. Electrode material properties for designing effective microbial electrosynthesis systems. J Mater Chem A. 2019;7(42):24420–36.
10. Izadi P, Fontmorin JM, Lim SS, Head IM, Yu EH. Enhanced bio-production from CO_2 by microbial electrosynthesis (MES) with continuous operational mode. Faraday Discuss. 2021;230:344–59.
11. Blasco-Gómez R, Batlle-Vilanova P, Villano M, Balaguer MD, Colprim J, Puig S. On the edge of research and technological application: A critical review of electromethanogenesis. Int J Mol Sci. 2017;18(4):1–32.
12. Carrillo-Peña D, Mateos R, Moran A, Escapa A. Reduced graphene oxide improves the performance of a methanogenic biocathode. Fuel. 2022;321:123957.
13. Pelaz G, Carrillo-Peña D, Morán A, Escapa A. Electromethanogenesis at medium-low temperatures: Impact on performance and sources of variability. Fuel. 2022;310:122336.
14. Aryal N, Ammam F, Patil SA, Pant D. An overview of cathode materials for microbial electrosynthesis of chemicals from carbon dioxide. Green Chem. 2017;19(24):5748–60.
15. Zhang T, Nie H, Bain TS, Lu H, Cui M, Snoeyenbos-west OL, et al. Improved cathode materials for microbial electrosynthesis. Energy Environ Sci. 2013;6:217–24.
16. Guo K, Prévoteau A, Patil SA, Rabaey K. Engineering electrodes for microbial electrocatalysis. Curr Opin Biotechnol. 2015;33:149–56.
17. Kerzenmacher S. Engineering of microbial electrodes. Adv Biochem Eng Biotechnol. 2019;167:135–80.
18. Mateos R, Alonso RM, Escapa A, Morán A. Methodology for fast and facile characterisation of carbon-based electrodes focused on bioelectrochemical systems development and scale up. Materials (Basel). 2017;0(79):1–11.
19. Wei J, Liang P, Huang X. Recent progress in electrodes for microbial fuel cells. Bioresour Technol. 2011;102:9335–44.
20. Song X, Huang L, Lu H, Zhou P, Wang M, Li N. An external magnetic field for efficient acetate production from inorganic carbon in Serratia marcescens catalyzed cathode of microbial electrosynthesis system. Biochem Eng J. 2020;155:107467.
21. Alqahtani MF, Bajracharya S, Katuri KP, Ali M, Xu J, Alarawi MS, et al. Enrichment of salt-tolerant CO_2–fixing communities in microbial electrosynthesis systems using porous ceramic hollow tube wrapped with carbon cloth as cathode and for CO_2 supply. Sci Total Environ. 2021;766:142668.
22. Li Z, Cai J, Gao Y, Zhang L, Liang Q, Hao W, et al. Efficient production of medium chain fatty acids in microbial electrosynthesis with simultaneous bio-utilization of carbon dioxide and ethanol. Bioresour Technol. 2022;352:127101.
23. Wang H, Du H, Xie H, Zhu J, Zeng S, Igarashi Y, et al. Dual-chamber differs from single-chamber microbial electrosynthesis in biogas production performance under low temperature (15°C). Bioresour Technol. 2021;337:125377.
24. Rojas MDPA, Zaiat M, González ER, De Wever H, Pant D. Enhancing the gas–liquid mass transfer during microbial electrosynthesis by the variation of CO_2 flow rate. Process Biochem. 2021;101:50–8.
25. Fonseca EU, Yang W, Wang X, Rossi R, Logan BE. Comparison of different chemical treatments of brush and flat

carbon electrodes to improve performance of microbial fuel cells. Bioresour Technol. 2021;342:125932.
26. Lee M, Nagendranatha Reddy C, Min B. In situ integration of microbial electrochemical systems into anaerobic digestion to improve methane fermentation at different substrate concentrations. Int J Hydrogen Energy. 2019;44:2380–9.
27. Yang HY, Bao BL, Liu J, Qin Y, Wang YR, Su KZ, et al. Temperature dependence of bioelectrochemical CO_2 conversion and methane production with a mixed-culture biocathode. Bioelectrochemistry. 2018;119:180–8.
28. Catania C, Karbelkar AA, Furst AL. Engineering the interface between electroactive bacteria and electrodes. Joule. 2021;5(4):743–7.
29. Van Eerten-Jansen MCAA, Veldhoen AB, Plugge CM, Stams AJM, Buisman CJN, Ter Heijne A. Microbial community analysis of a methane-producing biocathode in a bioelectrochemical system. Archaea. 2013;2013:481784.
30. Carrillo-Peña D, Escapa A, Hijosa-Valsero M, Paniagua-García AI, Díez-Antolínez R, Mateos R. Bioelectrochemical enhancement of methane production from exhausted vine shoot fermentation broth by integration of MEC with anaerobic digestion. Biomass Convers Biorefinery. 2022;1–10. https://doi.org/10.1007/s13399-022-02890-7
31. American Public Health Association, American Water Works Association, Water Environment Federation. Standard methods for the examination of water and wastewater. 22nd ed. In: Baird RB, Rice EW, Eaton AD, Clesceri LS, editors. Washington, DC: American Public Health Association; 2012.
32. Bajracharya S, Ter Heijne A, Dominguez Benetton X, Vanbroekhoven K, Buisman CJN, Strik DPBTB, et al. Carbon dioxide reduction by mixed and pure cultures in microbial electrosynthesis using an assembly of graphite felt and stainless steel as a cathode. Bioresour Technol. 2015;195:14–24.
33. Ramírez-Guzmán A, Taran Y, Armienta MA. Geochemistry and origin of high-pH thermal springs in the Pacific coast of Guerrero, Mexico. Geofis Int. 2004;43(3): 415–25.
34. Wang Q, Garrity GM, Tiedje JM, Cole JR. Naïve Bayesian classifier for rapid assignment of rRNA sequences into the new bacterial taxonomy. Appl Environ Microbiol. 2007;73(16):5261–7.
35. Vassilev I, Dessì P, Puig S, Kokko M. Cathodic biofilms – A prerequisite for microbial electrosynthesis. Bioresour Technol. 2022;348:126788.
36. Cai W, Cui K, Liu Z, Jin X, Chen Q, Guo K, et al. An electrolytic-hydrogen-fed moving bed biofilm reactor for efficient microbial electrosynthesis of methane from CO2. Chem Eng J. 2022;428:132093.
37. Mohanakrishna G, Seelam JS, Vanbroekhoven K, Pant D. An enriched electroactive homoacetogenic biocathode for the microbial electrosynthesis of acetate through carbon dioxide reduction. Faraday Discuss. 2015;183:445–62.
38. Guneratnam AJ, Ahern E, FitzGerald JA, Jackson SA, Xia A, Dobson ADW, et al. Study of the performance of a thermophilic biological methanation system. Bioresour Technol. 2017;225:308–15.
39. Jourdin L, Lu Y, Flexer V, Keller J, Freguia S. Biologically induced hydrogen production drives high rate/high efficiency microbial electrosynthesis of acetate from carbon dioxide. ChemElectroChem. 2016;3(4):581–91.
40. Boas JV, Peixoto L, Oliveira VB, Simões M, Pinto AMFR. Cyclic voltammetry study of a yeast-based microbial fuel cell. Bioresour Technol Reports. 2022;17:100974.
41. Song YE, Mohamed A, Kim C, Kim M, Li S, Sundstrom E, et al. Biofilm matrix and artificial mediator for efficient electron transport in CO_2 microbial electrosynthesis. Chem Eng J. 2022;427:131885.
42. Xiao S, Fu Q, Xiong K, Li Z, Li J, Zhang L, et al. Parametric study of biocathodes in microbial electrosynthesis for CO_2 reduction to CH_4 with a direct electron transfer pathway. Renew Energy. 2020;162:438–46.
43. Rozendal RA, Jeremiasse AW, Hamelers HVM, Buisman CJN. Hydrogen production with a microbial biocathode. Environ Sci Technol. 2008;42(2):629–34.
44. Costa KC and Leigh JA. Metabolic versatility in methanogens. Curr Opin Biotechnol. 2014;29(1):70–5.
45. Xu J, Sheng GP, Ma Y, Wang LF, Yu HQ. Roles of extracellular polymeric substances (EPS) in the migration and removal of sulfamethazine in activated sludge system. Water Res. 2013;47(14):5298–306.
46. Bin T, ShaoFeng Z, Yi W, BeiPing Z, LiHua Z, Yong Y. Molecular insight into electron transfer properties of extracellular polymeric substances of electroactive bacteria by surface-enhanced Raman spectroscopy. Sci China. 2019;62(10):1679–87.
47. Siegert M, Yates MD, Spormann AM, Logan BE. Methanobacterium dominates biocathodic archaeal communities in methanogenic microbial electrolysis cells. ACS Sustain Chem Eng. 2015;3:1668–76.
48. Mateos R, Escapa A, San-Martín MI, De Wever H, Sotres A, Pant D. Long-term open circuit microbial electrosynthesis system promotes methanogenesis. J Energy Chem. 2020;41:3–6.
49. Zheng S, Li M, Liu Y, Liu F. Desulfovibrio feeding methanobacterium with electrons in conductive methanogenic aggregates from coastal zones. Water Res. 2021;202:117490.
50. Li J, Li Z, Xiao S, Fu Q, Kobayashi H, Zhang L, et al. Startup cathode potentials determine electron transfer behaviours of biocathodes catalysing CO_2 reduction to CH_4 in microbial electrosynthesis. J CO2 Util. 2020;35:169–75.
51. Guo J, Peng Y, Ni BJ, Han X, Fan L, Yuan Z. Dissecting microbial community structure and methane-producing pathways of a full-scale anaerobic reactor digesting activated sludge from wastewater treatment by metagenomic sequencing. Microb Cell Fact. 2015;14:1–11.
52. Kobayashi H, Saito N, Fu Q, Kawaguchi H, Vilcaez J, Wakayama T, et al. Bio-electrochemical property and phylogenetic diversity of microbial communities associated with bioelectrodes of an electromethanogenic reactor. J Biosci Bioeng. 2013;116:114–7.
53. Flores-Rodriguez C and Min B. Enrichment of specific microbial communities by optimum applied voltages for enhanced methane production by microbial electrosynthesis in anaerobic digestion. Bioresour Technol. 2020;300:122624.
54. Noori MT, Vu MT, Ali RB, Min B. Recent advances in cathode materials and configurations for upgrading methane in bioelectrochemical systems integrated with anaerobic digestion. Chem Eng J. 2020;392:123689.
55. Di Capua F, Pirozzi F, Lens PNL, Esposito G. Electron donors for autotrophic denitrification. Chem Eng J. 2019;362:922–37.

56. Virdis B, Read ST, Rabaey K, Rozendal RA, Yuan Z, Keller J. Biofilm stratification during simultaneous nitrification and denitrification (SND) at a biocathode. Bioresour Technol. 2011;102:334–41.
57. Saheb-Alam S, Persson F, Wilén BM, Hermansson M, Modin O. A variety of hydrogenotrophic enrichment cultures catalyse cathodic reactions. Sci Rep. 2019;9:1–13.
58. Bambauer A, Rainey FA, Stackebrandt E, Winter J. Characterization of Aquamicrobium defluvii gen. nov. sp. nov., a thiophene-2-carboxylate-metabolizing bacterium from activated sludge. Arch Microbiol. 1998;169:293–302.
59. Zheng D, Gu W, Zhou Q, Zhang L, Wei C, Yang Q, et al. Ammonia oxidation and denitrification in a bio-anode single-chambered microbial electrolysis cell. Bioresour Technol. 2020;310:123466.
60. Ding H, Liu T, Hu Q, Liu M, Cai M, Jiang Y, et al. Effect of microbial community structures and metabolite profile on greenhouse gas emissions in rice varieties. Environ Pollut. 2022;306:119365.
61. Yi Y, Wang HZ, Chen YT, Gou M, Xia ZY, Hu B, et al. Identification of novel butyrate- and acetate-oxidizing bacteria in butyrate-fed mesophilic anaerobic chemostats by DNA-based stable isotope probing. Microb Ecol. 2020;79:285–98.
62. Wu Z, Nguyen D, Lam TYC, Zhuang H, Shrestha S, Raskin L, et al. Synergistic association between cytochrome bd-encoded Proteiniphilum and reactive oxygen species (ROS)-scavenging methanogens in microaerobic-anaerobic digestion of lignocellulosic biomass. Water Res. 2021;190:116721.
63. Aulenta F, Catapano L, Snip L, Villano M, Majone M. Linking bacterial metabolism to graphite cathodes: electrochemical insights into the H_2-producing capability of Desulfovibrio sp. ChemSusChem. 2012;5:1080–5.
64. Xiang Y, Liu G, Zhang R, Lu Y, Luo H. Acetate production and electron utilization facilitated by sulfate-reducing bacteria in a microbial electrosynthesis system. Bioresour Technol. 2017;241:821–9.

Celia De la Puente

Celia De la Puente is a Biotechnology student and researcher in the Chemical and Environmental Bioprocess Engineering Group at the University of León. Her work focuses on the study of microbial communities in biocathodes of bioelectrochemical systems.

Daniela Carrillo-Peña

Daniela Carrillo-Peña is a Chemical Engineer and currently a PhD student at the University of León, Spain. Her research focuses on bioelectrochemical systems: biocathodes for CO_2 capture and production of organic valuable chemicals, and bioanodes for organic wastewater treatment.

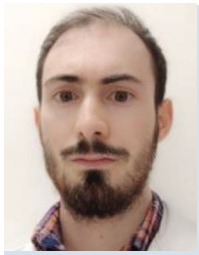

Guillermo Pelaz

Guillermo Pelaz is an Environmental Scientist and master's degree in Microbiology. He is currently a PhD student at the University of León. His research focuses on the use of biocathodes for energy surplus exploitation and biogas upgrading via microbial electrosynthesis.

Antonio Morán

Antonio Morán is a chemical engineer and holds PhD in chemical engineering at the University of Oviedo. He is a Full Professor at the University of León. His research is carried on Bioprocesses and Environmental Engineering, focusing on valuable chemicals and energy production and recovery.

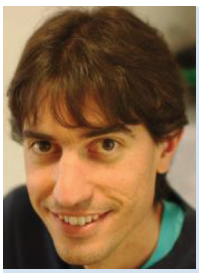

Raúl Mateos

Raúl Mateos is a Chemical Engineer, MEng in Renewable Energies and PhD in Chemical Engineering. He is currently an assistant professor at the University of León. His research is focused on CO_2 capture and utilisation for the production of value-added chemicals via Microbial Electrosynthesis.